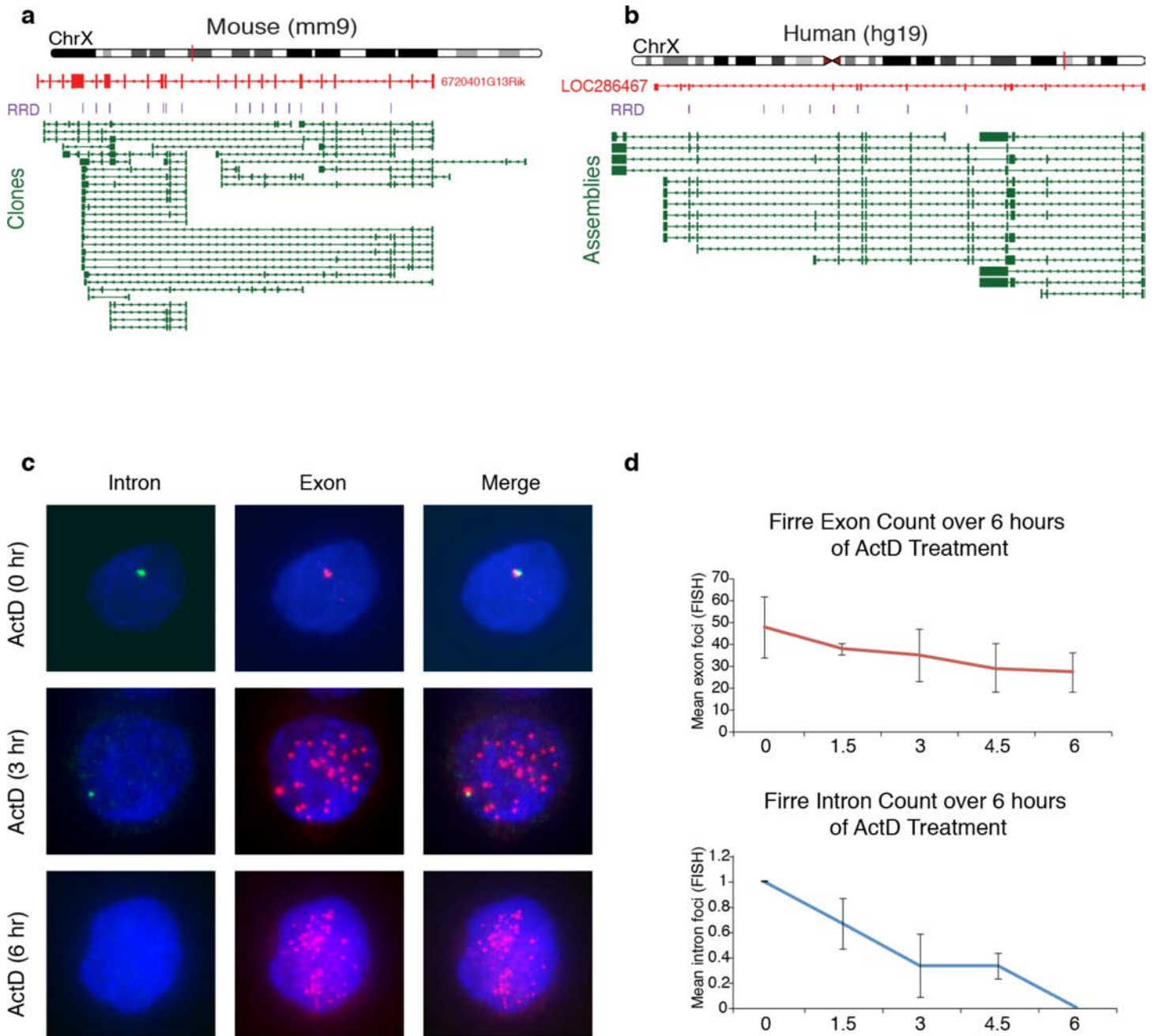
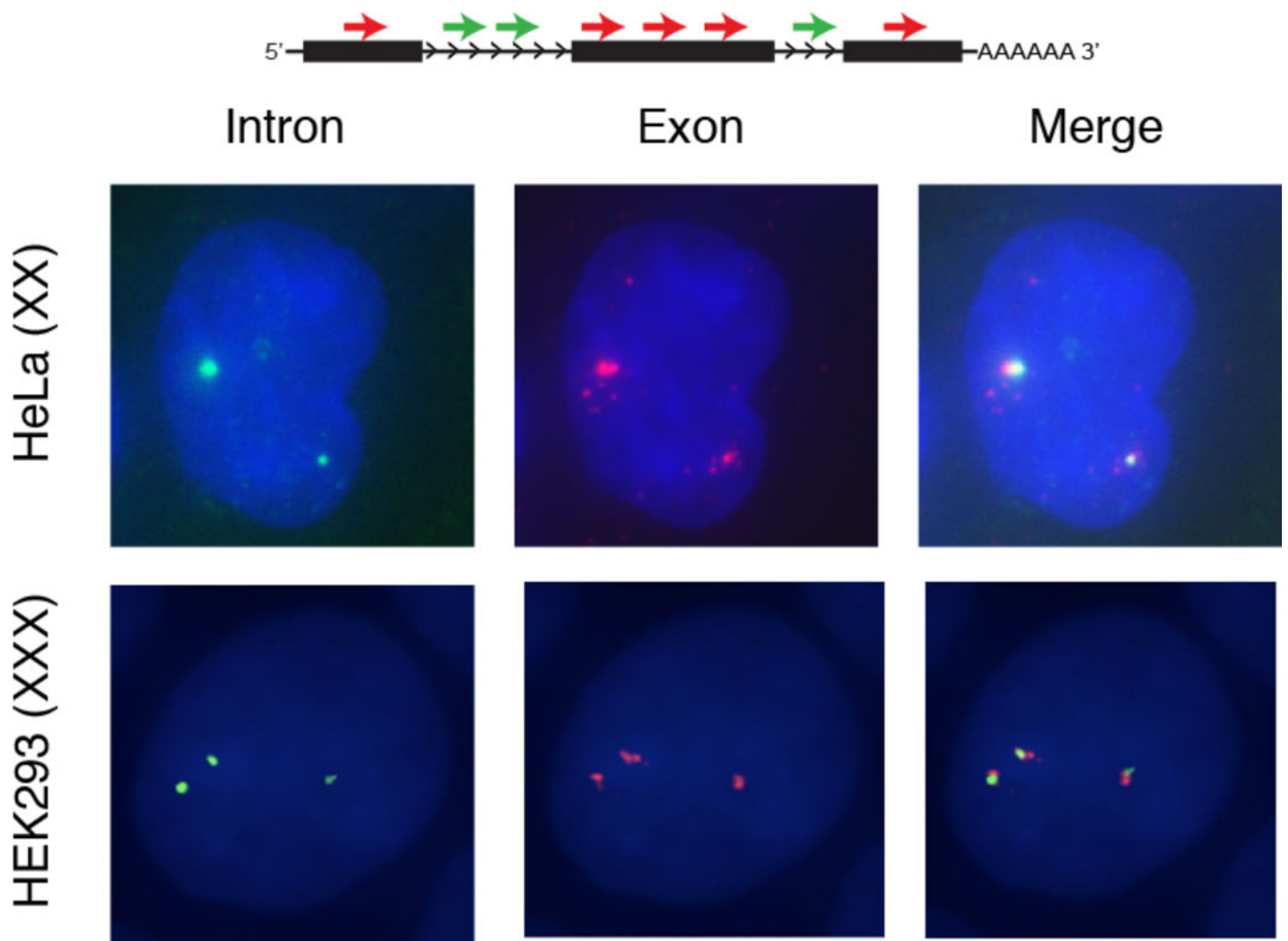


Topological Organization of Multi-chromosomal Regions by *Firre*

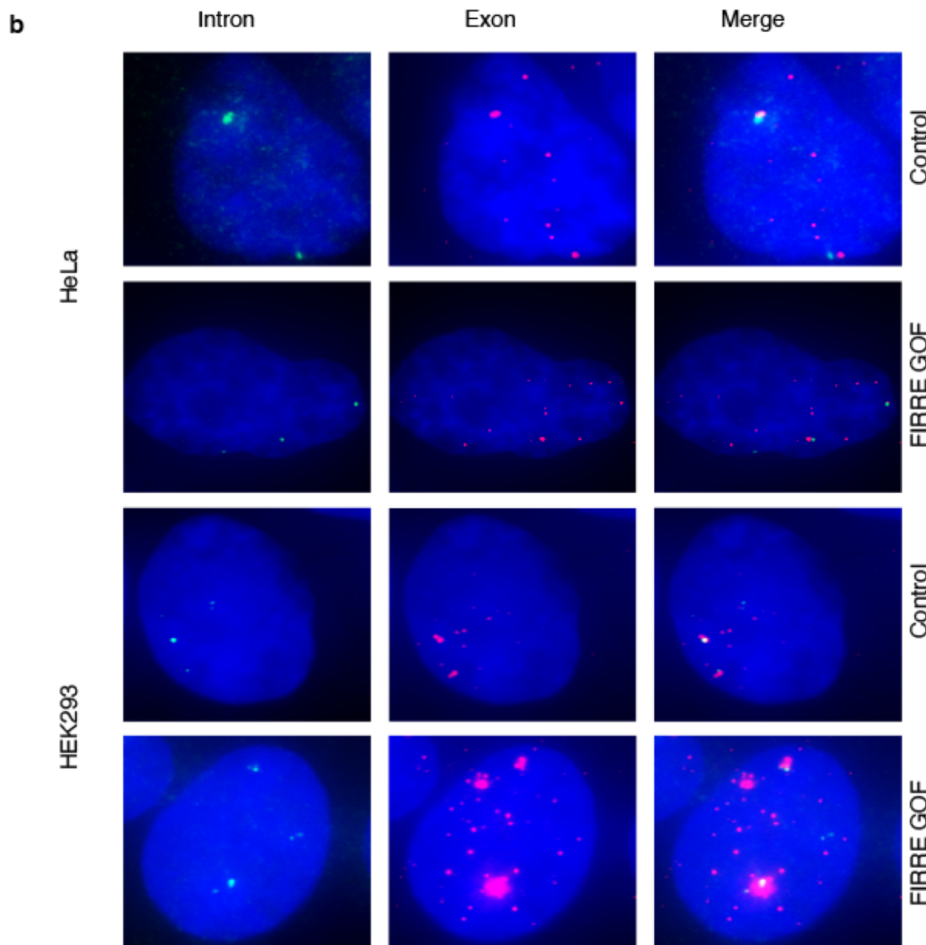
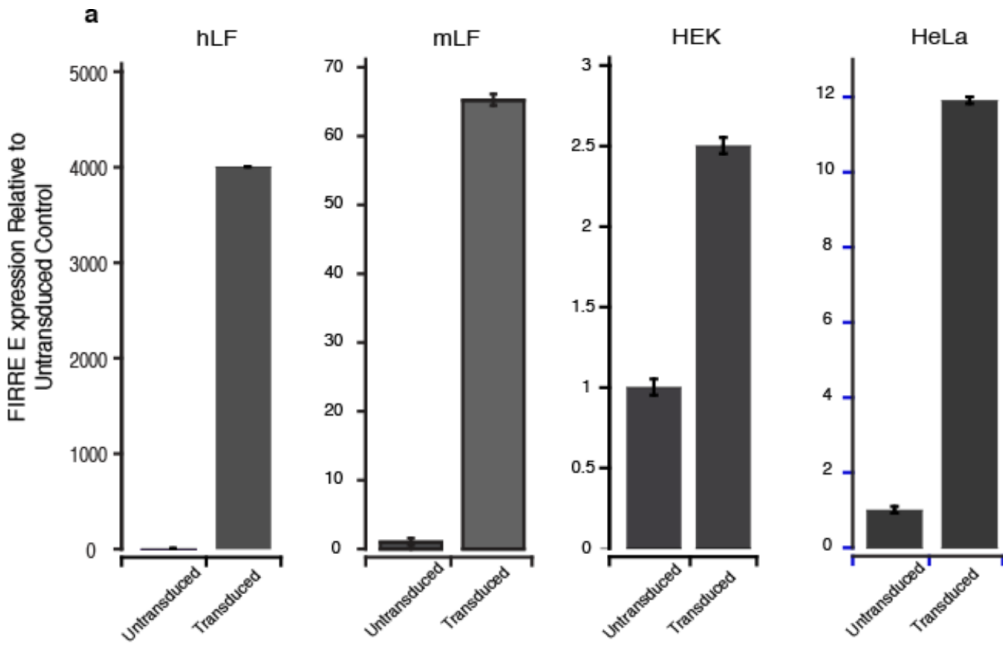
Ezgi Hacısuleyman^{1,2,3,13}, Loyal A. Goff^{2,3,4,13}, Cole Trapnell^{2,3}, Adam Williams⁵, Jorge Henao-Mejia⁵, Lei Sun⁶, Patrick McClanahan⁷, David G. Hendrickson^{2,3}, Martin Sauvageau^{2,3}, David R. Kelley^{2,3}, Michael Morse³, Jesse Engreitz³, Eric S. Lander³, Mitch Guttman⁸, Harvey F. Lodish^{6,9,10}, Richard Flavell^{5,11}, Arjun Raj⁷, and John L. Rinn^{2,3,12,14}.



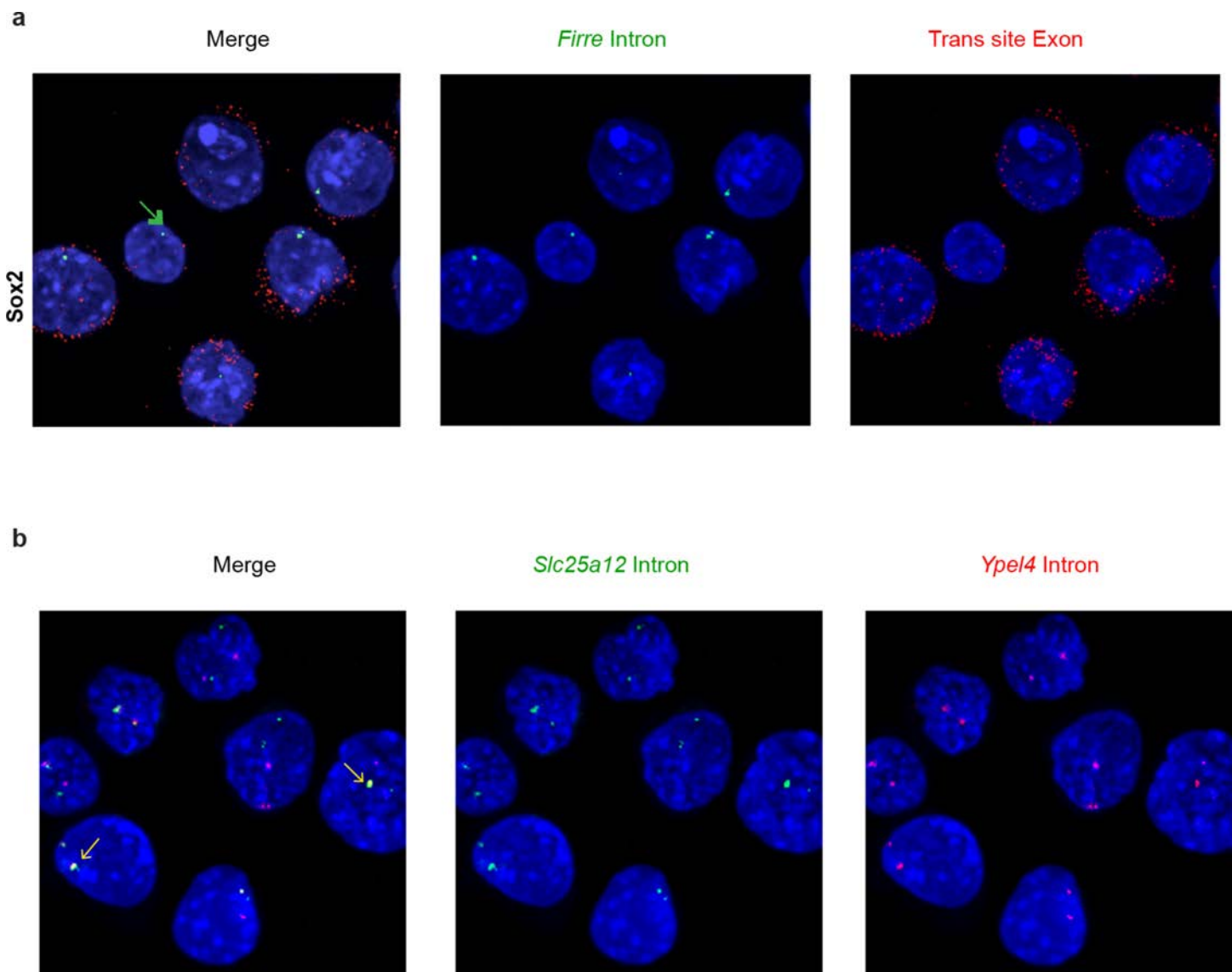
Supplementary Figure 1: Firre is a stable transcript. (a) Cloning of 50 different mouse isoforms of Firre, with most exons demarcated by the inclusion of the repeat domain RRD (purple tracks). (b) The isoform assemblies for human FIRRE are shown, again with most exons marked by RRD (purple marks). (c) Actinomycin-D treatment of male mESCs followed by RNA FISH for Firre over a course of 6 hours. (d) The number of nascent versus mature transcripts counted by image processing in Matlab.



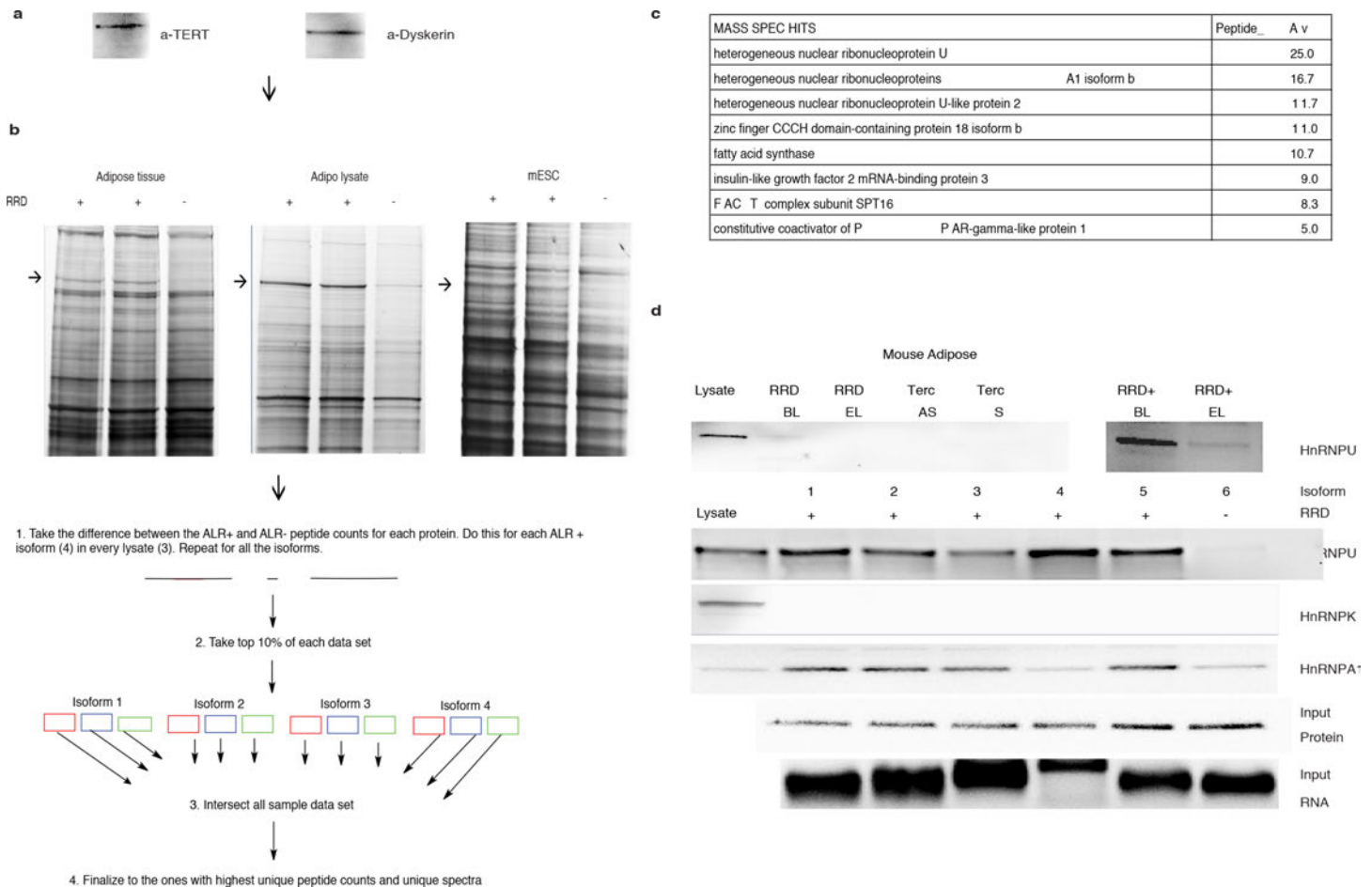
Supplementary Figure 2: Firre is a strictly nuclear lncRNA. Single molecule RNA fluorescence *in situ* hybridization (FISH) in HEK293s and HeLa cells, with introns labeled in “green” and exons in “red”, as described in Raj *et al.* (2008).



Supplementary Figure 3: Firre RNA is sufficient to form ectopic expression domains. (a) qRT-PCR analysis of the viral overexpression of the human isoform of FIRRE in HEK293, HeLa, and human lung fibroblasts (hLF), and the mouse isoform of Firre in mouse lung fibroblasts (mLF). Normalized to untransduced samples after all CT values are normalized to Gapdh. **(b)** Single molecule RNA FISH in transduced HeLa and HEK293 cells, which have endogenous Firre expression; introns labeled in “green” and exons in “red”

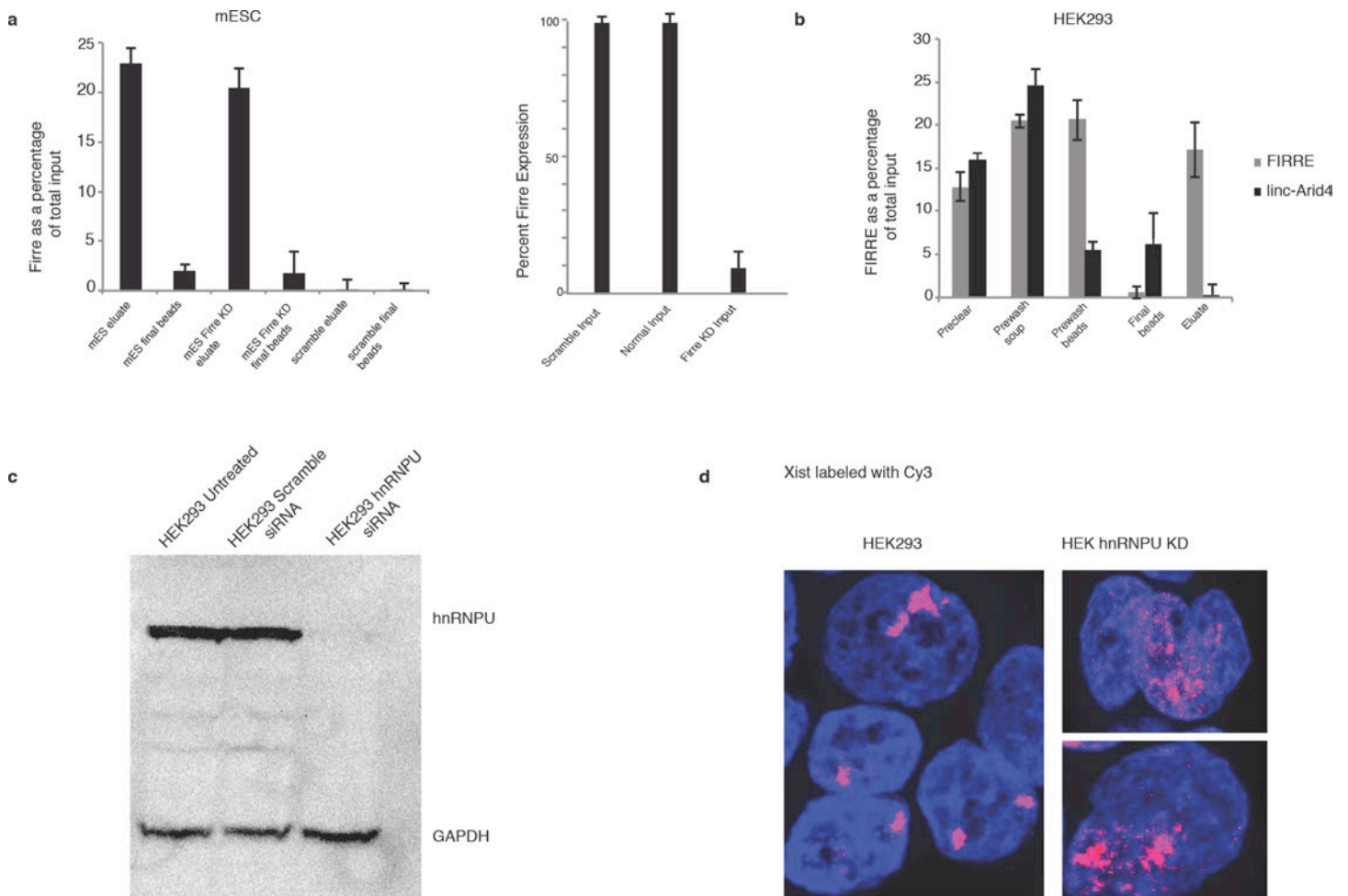


Supplementary Figure 4: Firre forms trans-chromosomal contacts. (a) Genes that were not detected to be bound by Firre by RAP were used as negative controls for FISH. Firre intron is shown in “green” and Sox2 exons are shown in “red.” **(b)** RNA co-FISH between the trans targets of Firre: Slc25a12 and Ypel4 (yellow arrows for co-localization): Slc25a12 intron in “green” and Ypel4 intron in “red.”



Supplementary Figure 5: Firre interacts with hnRNPU in mouse ES and adipose contexts. (a)

The RNA pull-down technique was developed and optimized by testing known lncRNA-protein interactions. For optimization, telomerase RNA TERC was chosen as well as others, such as SRP and 7SK (data not shown). The binding partners of TERC, Dyskerin and TERT, were recovered with high efficiency and specificity. (b) The optimized RNA pull-down technique was used to find the binding partners of Firre. The analysis of mass spectrometry data is outlined. (c) Based on the highest unique peptide counts across different isoforms and lysate conditions, we identified 8 candidate proteins that physically associate with Firre in an RRD-dependent manner. The top candidate was hnRNPU. (d) Firre interacts with hnRNPU in mouse adipose tissue as well as in mESC lysate. Western blots are shown for the pull-downs using *in vitro* biotinylated isoforms of Firre: five with RRD and one without. We compared end labeling (EL) and body labeling (BL) to exclude the possibility of a bias in binding and used TERC antisense (AS) and sense (S) as negative controls. hnRNPK and A1 are shown for RRD-specific interactions. 20% of the input protein lysate was loaded in the first lane for each Western blot. Input protein lysate and input RNA are included as loading controls.



Supplementary Figure 6: Firre-hnRNPU interaction is biologically relevant, and hnRNPU has a previously shown role in Xist localization. (a) Endogenous Firre was captured by desthiobiotin-modified DNA oligos in mESCs. The efficiency of capture was measured by qRT-PCR by comparing the RNA levels in the eluate and what is left on the beads post-elution after normalizing to 10% of the total input. The specificity of capture was measured by comparing the eluates from the targeting and scramble oligos. The endogenous RNA pull-down was repeated in mESCs, in which Firre was knocked down to test the specificity of the oligo for the RNA. (b) The endogenous pull-down was repeated in HEK293s to test for the human FIRRE. Additionally, specificity of the oligo was tested by measuring the elutions for the enrichment or depletion of an unrelated lincRNA, linc-Arid4a. (c) Western blot of HEK293 lysates before and after transfection with siRNAs targeting hnRNPU and scramble siRNAs. (d) RNA FISH of Xist in HEK293s after siRNA-mediated depletion of hnRNPU.

a

Figure 6A, panel 1 (left)



Figure 6A, panel 1 (right)



Figure 6A, panel 2

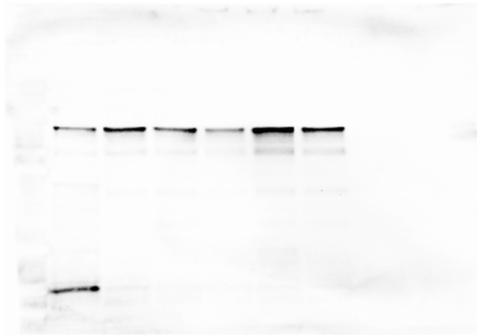


Figure 6A, panel 3

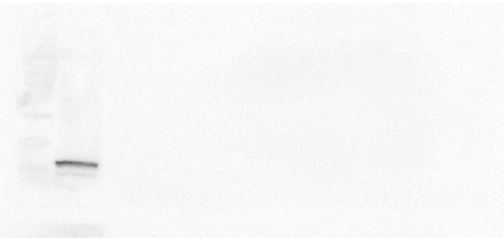
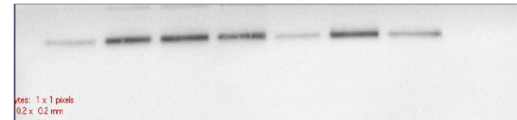


Figure 6A, panel 4



b

Figure 6B, panel 1

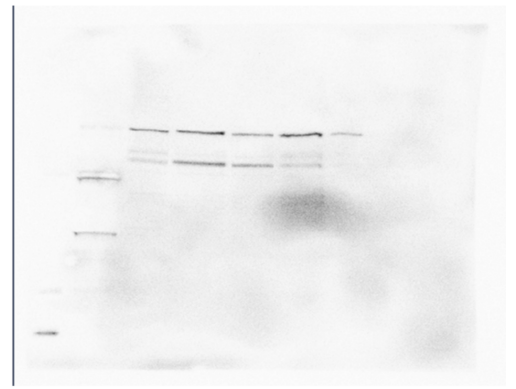


Figure 6B, panel 2

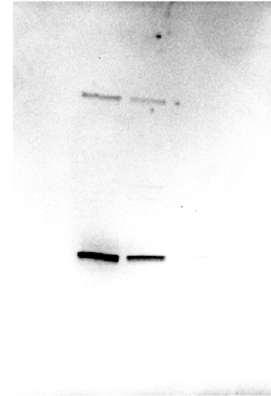
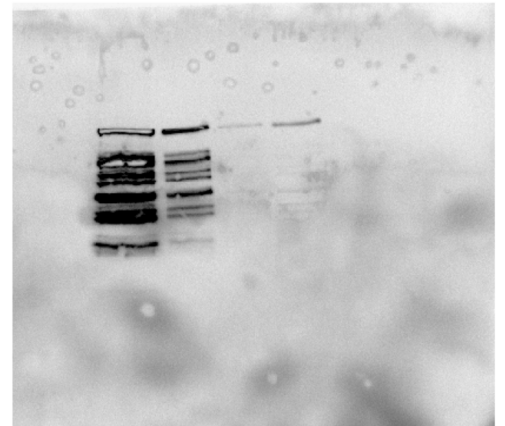


Figure 6B, panel 4



Supplementary Figure 7: Uncropped versions of Figure 6 A and 6B.

Supplementary References:

47. Price, A.L., Jones, N.C. & Pevzner, P.A. De novo identification of repeat families in large genomes. *Bioinformatics* **21 Suppl 1**, i351-8 (2005).
48. Donohoe, M.E., Silva, S.S., Pinter, S.F., Xu, N. & Lee, J.T. The pluripotency factor Oct4 interacts with Ctf and also controls X-chromosome pairing and counting. *Nature* **460**, 128-U147 (2009).
49. Kent, W.J. BLAT--the BLAST-like alignment tool. *Genome Res* **12**, 656-64 (2002).
50. Bradley, R.K. et al. Fast Statistical Alignment. *Plos Computational Biology* **5**(2009).
51. Arlotta, P. et al. Neuronal subtype-specific genes that control corticospinal motor neuron development in vivo. *Neuron* **45**, 207-221 (2005).
52. Tiveron, M.C., Hirsch, M.R. & Brunet, J.F. The expression pattern of the transcription factor Phox2 delineates synaptic pathways of the autonomic nervous system. *J Neurosci* **16**, 7649-60 (1996).
53. Guttman, M. et al. Ab initio reconstruction of cell type-specific transcriptomes in mouse reveals the conserved multi-exonic structure of lincRNAs. *Nat Biotechnol* **28**, 503-10 (2010).
54. Quinlan, A.R. & Hall, I.M. BEDTools: a flexible suite of utilities for comparing genomic features. *Bioinformatics* **26**, 841-2 (2010).
55. Vizlin-Hodzic, D., Johansson, H., Ryme, J., Simonsson, T. & Simonsson, S. SAF-A Has a Role in Transcriptional Regulation of Oct4 in ES Cells Through Promoter Binding. *Cellular Reprogramming* **13**, 13-27 (2011).
56. Trapnell, C. et al. Differential gene and transcript expression analysis of RNA-seq experiments with TopHat and Cufflinks. *Nat Protoc* **7**, 562-78 (2012).
57. Kelley, D. & Rinn, J. Transposable elements reveal a stem cell-specific class of long noncoding RNAs. *Genome Biol* **13**, R107 (2012).
58. Trapnell, C., Pachter, L. & Salzberg, S.L. TopHat: discovering splice junctions with RNA-Seq. *Bioinformatics* **25**, 1105-11 (2009).
59. Trapnell, C. et al. Differential analysis of gene regulation at transcript resolution with RNA-seq. *Nat Biotechnol* **31**, 46-53 (2013).
60. Subramanian, A. et al. Gene set enrichment analysis: a knowledge-based approach for interpreting genome-wide expression profiles. *Proc Natl Acad Sci U S A* **102**, 15545-50 (2005).